Spontaneous Asymmetry of Coated Spherical Nanoparticles in Solution and at Liquid-Vapor Interfaces

J. Matthew D. Lane* and Gary S. Grest†

Sandia National Laboratories, Albuquerque, New Mexico 87185, USA

(Received 23 February 2010; published 9 June 2010)

Spherical nanoparticles (NPs), uniformly coated with a simple polymer used to passivate NPs in solution, are shown to produce highly asymmetric coating arrangements. We show that a class of spherical particles is not symmetrically coated even when extremely uniform grafting arrangements and full coverages are employed. We demonstrate, using explicit-atom molecular dynamics simulations of model NPs, that geometric properties dictate when a coating's spherical symmetry will be unstable and show that the chain end group and the solvent play a secondary role in determining the properties of surface patterns. At the water-vapor interface the coatings are significantly distorted and oriented by the surface. These asymmetric and oriented coatings are expected to have a dramatic effect on the interactions between NPs and will likely influence the structures of aggregated NPs which self-assemble in the bulk and at surfaces.

DOI: 10.1103/PhysRevLett.104.235501 PACS numbers: 81.16.Dn, 62.25.−g, 81.07.−b, 83.80.Qr

Aggregation of nanoparticles (NPs) in suspensions is an obstacle to their commercial and industrial use. Coating NPs with short-chain polymer coatings has proven to be a simple and effective way to stabilize NP suspensions for bulk handling. Understanding the interactions between NPs and how these are affected by the presence of solvents is therefore of significant practical importance for controlling NP suspension rheology and self-assembly.

Short-chain soft polymer-coated particles and star polymers are often modeled using surface-integrated interactions such as Gauss-core interactions [1–3]. However, our recent simulations of polyethylene-oxide-coated silica [4] have raised questions about the applicability of spherically symmetric interactions for small NPs. Small NPs exhibit strong coating asymmetries and nonlinear responses which cannot be time-averaged away. Recent experiments [5] have shown that coated spherical NPs can self-assemble into a variety of extended anisotropic structures in a homopolymer matrix depending on the coating chain length and grafting density. Understanding the spontaneous asymmetries of spherical coatings and their effect on interactions between nanoparticles is therefore important for the study and control of self-assembly processes in the bulk and at evaporating interfaces [6,7].

Self-assembled thiol coatings on Au or Ag are relatively simple systems and have been well studied both by experiment [8,9] and by simulation as a general model system for coatings. Since Luedtke and Landman first reported simulations of passivated gold nanocrystallites [10], several groups have studied the structure and dynamics of the gold-thiol system. Computational studies of the chain mobility [11], chain dynamics [12], surface organization of the attached ligands [13], chain bundling [14], substrate interaction, and aggregate assemblies [10] have been conducted in the absence of explicit solvents.

In this Letter, we investigate the organization of simple alkanethiol coatings on Au NPs in dilute solutions of explicitly modeled water and decane for several combinations of chain length and termination. A rich response is observed, with chains organizing into diverse structures ranging from homogeneous to clustered and from spherically symmetric to highly anisotropic. We show that for certain combinations of particles and coatings, symmetry is not possible and stable surface patterning produces asymmetric coatings even for the most uniform grafting arrangements. The asymmetric response appears to be reinforced when particles are at a surface.

Alkanethiol-coated Au NPs are modeled with an all-atom representation. Three Au cores were constructed with diameters of 2.0, 4.0, and 8.0 nm at a coverage of 4.77 chains/nm^2, which gives 60, 240, and 960 chains per NP, respectively. The number of Au atoms N_{Au} was determined as in Leff *et al.* [15]. The sulfur head groups were grafted in a C_{60}, C_{240}, or C_{960} spherical fullerene arrangement [16], with chains, initially all-trans, oriented radially from the sulfur head group. The grafting density is taken from experiment [8], but the fullerene arrangement is an idealized uniform grafting model. In our previous studies [17] of alkanethiols on flat gold substrates, we used Klein and Hautman's integrated effective gold-thiol interaction potential [18]. However, here our particles are too small to justify a surface-integrated interaction. Since the Au core only weakly interacts with the alkanethiol coating and the solvent, they were not included explicitly. The mass of the Au atoms was distributed equally to the sulfur atoms. The sulfur atoms were treated as a rigid body which was allowed to translate and rotate. The ligands used in this study are 1-decanethiol S-$(CH_2)_9$-X, or 1-octadecanethiol S-$(CH_2)_{17}$-X, where $X = CH_3$ or COOH. The carboxylic acid is a weak acid with pKa from 4 to 5. For small systems, ionization is not expected to play a significant role. Our systems, with 10^1–10^3 COOH per system, are not

ionized. Although not addressed here, added salts could significantly screen the interactions of the partial charges in the COOH termination. Sandberg *et al.* address some of these issues in their study of spherical polyelectrolyte brushes [19].

The LAMMPS classical molecular dynamics code [20] was used with a Verlet integration time step of 1 fs. The coated NPs were initially equilibrated in an implicit solvent at 300 K with a Langevin thermostat with damping coefficient Γ of 0.01 fs^{-1}. This corresponds to an implicit poor solvent for both the alkane backbone and the terminal groups. Increasing the temperature improves the quality of the implicit solvent [13]. We extend previous implicit-solvent studies by modeling water and decane solvents explicitly. The OPLS-AA force field of Jorgensen and co-workers [21,22] was used with van der Waals interactions truncated at 1.0 nm. The TIP3P water model [23] was used with the SHAKE algorithm [24] applied to bonds and angles. Long-range Coulomb interactions were calculated with the fully periodic Particle-Particle Particle-Mesh method [25] for the bulk systems and with the 2D slab Particle-Particle Particle-Mesh method [26] for the liquid-vapor interface systems.

For the 2 and 4 nm diameter NPs, two bulk systems of initial size 15 nm $\times$ 15 nm $\times$ 20 nm consisting of 221 332 water molecules and 12 800 decane molecules were generated. After equilibration, a spherical void just larger than the NP was grown to accommodate the NP. For the 8 nm diameter NPs, two larger systems of initial size 20 nm $\times$ 20 nm $\times$ 20 nm were used so that the NP did not interact with itself through the periodic boundaries. After the NPs were added to the systems, the simulations were run in an NPT ensemble at a pressure of 1 atm for 1.0 ns. The temperature was maintained by a Nosé-Hoover thermostat with a damping parameter of 0.01 fs^{-1}. In separate simulations, the NP was placed 0.3–0.5 nm above a water-vapor interface. The water-vapor systems were of size 15 nm $\times$ 15 nm $\times$ 20 nm and run in the NVT ensemble at 300 K for between 2.0 and 2.8 ns until the NPs came to equilibrium at the surface.

Dilute solutions.—Figures 1–3, show examples of equilibrated configurations for 2, 4, and 8 nm diameter NPs in dilute solutions, respectively. The figures show 12 structures, resulting from combinations of two chain lengths, two terminal groups, and three solvents. These are experimentally tunable variables; however, direct observation of their effects on the coating structure is currently only possible computationally. We discuss two characteristics of the particle coatings' response: first, the overall homogeneity of the surface distribution; second, the nature of patterning for inhomogeneous cases.

The primary driver for the surface inhomogeneity is the geometry of the spherical coatings. Unlike flat coatings, curvature means that chains have free volume to explore even when densely packed at their grafting point. The free volume per chain provided by the geometry is

$$\Delta v = \frac{V_{\text{sphere}} - V_{\text{flat}}}{\#\text{of chains}} = \frac{1}{3\sigma}\left[\frac{l^3}{r^2} + 3\frac{l^2}{r}\right], \qquad (1)$$

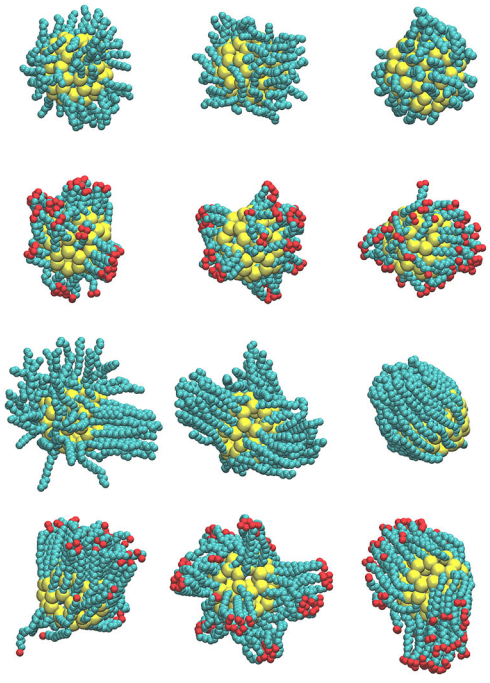

FIG. 1 (color online). The 2 nm diameter Au NPs with alkanethiol ligands equilibrated in (from left to right) decane, implicit solvent, and water for (from top to bottom) S-$(CH_2)_9$-CH_3, S-$(CH_2)_9$-COOH, S-$(CH_2)_{17}$-CH_3, and S-$(CH_2)_{17}$-COOH.

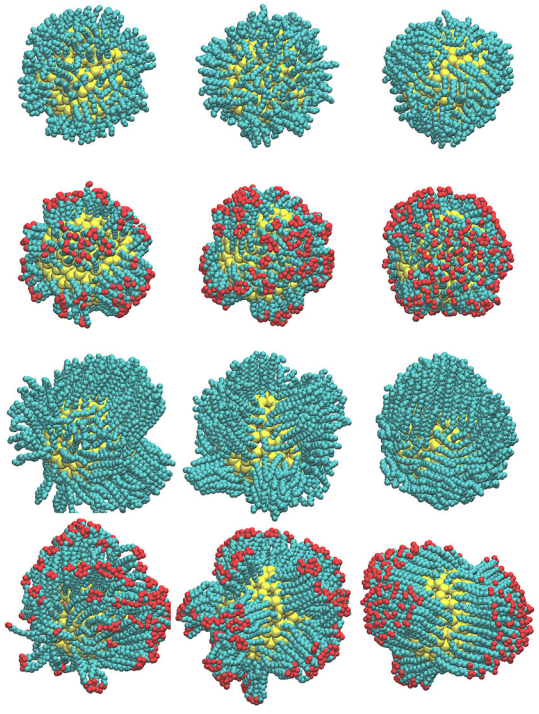

FIG. 2 (color online). The 4 nm diameter Au NPs with alkanethiol ligands equilibrated in (from left to right) decane, implicit solvent, and water for (from top to bottom) S-$(CH_2)_9$-CH_3, S-$(CH_2)_9$-COOH, S-$(CH_2)_{17}$-CH_3, and S-$(CH_2)_{17}$-COOH.

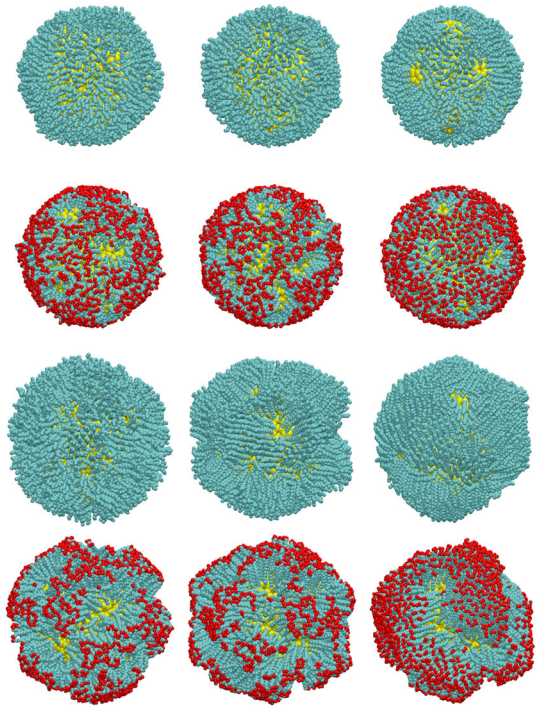

FIG. 3 (color online). The 8 nm diameter Au NPs with alkanethiol ligands equilibrated in (from left to right) decane, implicit solvent, and water for (from top to bottom) S-$(CH_2)_9$-CH_3, S-$(CH_2)_9$-COOH, S-$(CH_2)_{17}$-CH_3, and S-$(CH_2)_{17}$-COOH.

where $V_{\text{sphere}} = \frac{4}{3}\pi(l + r)^3 - \frac{4}{3}\pi r^3$ is the volume available to chains on a sphere, $V_{\text{flat}} = 4\pi r^2 l$ is the volume for the same area on a flat surface, σ is the surface density, r is the NP radius, and l is the chain length. Chain lengths were 1.4 nm and 2.4 nm for decanethiol and octadecanethiol.

Table I lists the free volume per chain, Δv, for the coated NPs. Also in Table I, the surface inhomogeneity of each coating is characterized by the standard deviation of the local density over the surface. The coated particles are listed in decreasing value of Δv, and the surface inhomogeneity follows within each combination of solvent and terminal group. The local density was calculated at ~2000 overlapping equal-area surface patches equally spaced over the sphere. Coating atoms contributed to the density calculation for a patch if they fell within a circular cone with a vertex at the NP center and an axis extending radially through the patch center. Each cone intersected the NP surface on a circle which inscribed a curved surface with the proper patch area. All coating atoms at any radius were considered. The standard deviation of the local density was used as a measure of surface inhomogeneity. A patch area of 0.785 nm^2 was chosen to be as small as possible, while ensuring every patch contained at least the mass equivalent of one chain. Since the standard deviation depends on patch size, it does not provide an absolute measure of inhomogeneity. However, for constant patch size, the relative values correspond to the relative homogeneity of the coatings. Values shown are instantaneous. A subset of the equilibrated particles were simulated for an additional ns, during which chain arrangements varied with time, but our measure of coating uniformity fluctuated by less than 5%.

TABLE I. Free volume per chain Δv and surface inhomogeneity measured as a standard deviation of the local surface density for coated Au NPs in dilute solvent.

D	Chain	Δv (nm^3)	Decane Standard deviation	Implicit Standard deviation	Water Standard deviation
2	S-$(CH_2)_{17}$-CH_3	0.844	59.5%	75.3%	68.2%
4	S-$(CH_2)_{17}$-CH_3	0.362	49.1%	52.5%	46.3%
2	S-$(CH_2)_9$-CH_3	0.252	31.5%	36.1%	32.4%
8	S-$(CH_2)_{17}$-CH_3	0.166	23.9%	38.7%	33.0%
4	S-$(CH_2)_9$-CH_3	0.115	23.8%	25.2%	33.3%
8	S-$(CH_2)_9$-CH_3	0.054	14.8%	17.4%	22.2%
2	S-$(CH_2)_{17}$-COOH	0.844	68.9%	55.1%	82.1%
4	S-$(CH_2)_{17}$-COOH	0.362	52.4%	59.6%	66.6%
2	S-$(CH_2)_9$-COOH	0.252	47.3%	50.6%	48.2%
8	S-$(CH_2)_{17}$-COOH	0.166	36.9%	42.3%	41.8%
4	S-$(CH_2)_9$-COOH	0.115	34.9%	41.6%	33.8%
8	S-$(CH_2)_9$-COOH	0.054	22.1%	27.6%	19.7%

Table I shows that the free volume per chain determines the relative uniformity of the surface distribution for a given termination and solvent. This explains the general observations that the smaller diameter NPs have coatings which are most strongly asymmetric, and that the ligands become visibly more symmetric as the diameter increases, especially for short chains. However, geometric considerations can be overwhelmed by solvent-ligand or ligand-ligand interactions. For example, Ghorai *et al.* [13] showed that uniform distributions can always be attained with sufficiently high temperatures.

More qualitatively, certain patterns are apparent in the images of the NPs. There is, for instance, more segregation with hydrophilic carboxyl termination than with the hydrophobic methyl termination in all solvents. In water, the carboxyl groups segregate into large islands, while in the poor implicit solvent and decane, they form tighter, but smaller clusters. These patterns show themselves in the density variation on the surface as well. Table I shows that the hydrophilic carboxyl groups have higher density variations than the methyl in almost every geometry. These patterns reflect the interplay between chain backbone, chain termination, and solvent interactions.

Liquid-vapor interfaces.—Intriguingly, the anisotropic NP coatings seen in bulk solvents appear to be reinforced by interactions at the interface. Figure 4 shows the results of our simulations for 12 Au NPs (described above) at the water-vapor interface.

As in the dilute solution case, the coating shape depends strongly on the amount of free volume provided by the geometry, end group, and solvent properties. Unlike in the bulk, here any inhomogeneity or asymmetry tends to orient with the surface so as to minimize free energy. For in-

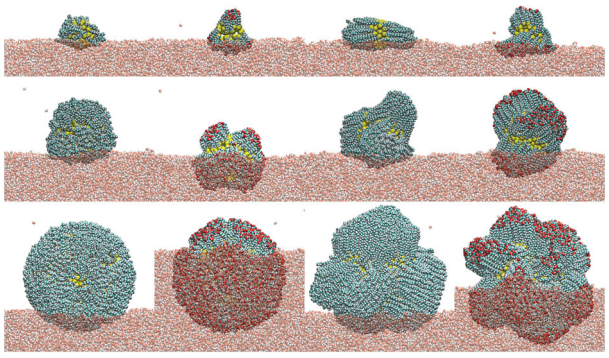

FIG. 4 (color online). Equilibrated polymer-coated alkanethiol NPs of diameter (from top to bottom) 2.0, 4.0, and 8.0 nm at the water-vapor interface for S-$(CH_2)_9$-CH_3, S-$(CH_2)_9$-COOH, S-$(CH_2)_{17}$-CH_3, and S-$(CH_2)_{17}$-COOH (from left to right).

stance, in the smallest particles coated with COOH-terminated ligands, the carboxyl-terminated chains form elongated structures with the -COOH ends bundled together. In the presence of the water interface, a somewhat rodlike particle with a hydrophobic center and hydrophilic ends develops with one hydrophilic end buried in the solvent and the other extending out of the interface. For the smallest particles coated with CH_3-terminated ligands, a similar rodlike shape develops, but here lays in the plane of the interface. There is little penetration into the water, and most of the ligands are in contact with the vapor. As in the bulk, larger particles and shorter chains tend to form more homogeneous coatings which have no preferred orientation at the surface. For COOH-terminated coatings, these homogeneous configurations are more likely to be fully water miscible.

We also studied 2.6 nm NPs at the liquid-vapor interface of decane. The CH_3-terminated NPs are miscible and do not remain at the surface. The COOH-terminated NPs are similar to the structures shown in the top row of Fig. 4 except that the NPs are almost completely submerged, with only the tip of the upper bundle of COOH-terminated NPs exposed to the vapor.

We have shown that spherical NPs, uniformly coated with an alkanethiol polymer, produce highly asymmetric coating arrangements in solution. Moreover, there is a class of spherical particles which cannot be symmetrically coated to prevent aggregation, even when extremely uniform grafting arrangements and full coverages are employed. Geometric properties can be reduced to a single parameter, the free volume per chain, which dictates when a coating's spherical symmetry will be unstable. The chain end group and the solvent play a secondary role in determining the properties of surface patterns. At the liquid-vapor interface the interaction with the asymmetric environment exaggerates and orients the asymmetric configuration of the ligand coatings for the smallest NPs. These asymmetric structures, both in the bulk and at the interface, are expected to have a dramatic effect on the NP/NP interactions. A study of aggregated structures with multiple particles is currently underway. We anticipate that the understanding of the higher-concentration solutions of these particles will lead to applications in controlled self-assembly of NPs, through coating manipulation.

The authors thank A. E. Ismail for discussions. This work was made possible by generous computer time at the New Mexico Computing Application Center and computations were performed, in part, at the Center for Integrated Nanotechnologies, a U.S. Department of Energy, Office of Basic Energy Sciences user facility. Sandia is a multiprogram laboratory operated by Sandia Corporation, a Lockheed Martin Company, for the U.S. Department of Energy under Contract No. DE-AC04-94AL85000.

*jlane@sandia.gov
†gsgrest@sandia.gov

[1] C. N. Likos *et al.*, J. Chem. Phys. **117**, 1869 (2002).
[2] C. N. Likos, Soft Matter **2**, 478 (2006).
[3] S. A. Baeurle and J. Kroener, J. Math. Chem. **36**, 409 (2004).
[4] J. M. D. Lane *et al.*, Phys. Rev. E **79**, 050501(R) (2009), and extended work in progress.
[5] P. Akcora *et al.*, Nature Mater. **8**, 354 (2009).
[6] Y. Min *et al.*, Nature Mater. **7**, 527 (2008).
[7] T. P. Bigioni *et al.*, Nature Mater. **5**, 265 (2006).
[8] G. H. Woehrle, L. O. Brown, and J. E. Hutchison, J. Am. Chem. Soc. **127**, 2172 (2005).
[9] M. C. Daniel and D. Astruc, Chem. Rev. **104**, 293 (2004).
[10] W. D. Luedtke and U. Landman, J. Phys. Chem. **100**, 13 323 (1996).
[11] B. J. Henz, T. Hawa, and M. R. Zachariah, Langmuir **24**, 773 (2008).
[12] S. Rapino and F. Zerbetto, Small **3**, 386 (2007).
[13] P. K. Ghorai and S. C. Glotzer, J. Phys. Chem. C **111**, 15 857 (2007).
[14] C. Singh *et al.*, Phys. Rev. Lett. **99**, 226106 (2007).
[15] D. V. Leff, P. C. Ohara, J. R. Heath, and W. M. Gelbart, J. Phys. Chem. **99**, 7036 (1995).
[16] B. I. Dunlap and R. R. Zope, Chem. Phys. Lett. **422**, 451 (2006).
[17] J. M. D. Lane, M. Chandross, M. J. Stevens, and G. S. Grest, Langmuir **24**, 5209 (2008).
[18] J. Hautman and M. L. Klein, J. Chem. Phys. **91**, 4994 (1989).
[19] D. J. Sandberg, J.-M. Y. Carrillo, and A. V. Dobrynin, Langmuir **23**, 12 716 (2007).
[20] S. Plimpton, J. Comput. Phys. **117**, 1 (1995).
[21] W. L. Jorgensen, D. S. Maxwell, and J. TiradoRives, J. Am. Chem. Soc. **118**, 11 225 (1996).
[22] E. K. Watkins and W. L. Jorgensen, J. Phys. Chem. A **105**, 4118 (2001).
[23] W. Jorgensen *et al.*, J. Chem. Phys. **79**, 926 (1983).
[24] J. P. Ryckaert, G. Ciccotti, and H. J. C. Berendsen, J. Comput. Phys. **23**, 327 (1977).
[25] R. W. Hockney and J. W. Eastwood, *Computer Simulation Using Particles* (Adam Hilger-IOP, Bristol, 1988).
[26] P. S. Crozier, R. L. Rowley, and D. Henderson, J. Chem. Phys. **114**, 7513 (2001).